Mediated Inner-Sphere Electron Transfer Induces Homogeneous Reduction of CO_2 via Through-Space Electronic Conjugation

Shelby L. Hooe[#[a]], Juan J. Moreno[#[a]], Amelia G. Reid[[a]], Emma N. Cook[[a]], and Charles W. Machan*[[a]]

[a] Department of Chemistry
University of Virginia
McCormick Road PO Box 400319
S.L.H. ORCID 0000-0002-6991-2273; J.J.M. ORCID 0000-0003-1809-6170; E.N.C. ORCID 0000-0002-0568-3600; A.G.R ORCID 0000-0002-2868-4091

* correspondence to: machan@virginia.edu; ORCID 0000-0002-5182-1138

\# These authors contributed equally to this work

Abstract: The electrocatalytic reduction of CO_2 is an appealing method for converting renewable energy sources into value-added chemical feedstocks. We report a co-electrocatalytic system for the reduction of CO_2 to CO comprised of a molecular Cr complex and dibenzothiophene-5,5-dioxide (DBTD) as a redox mediator which achieves high activity (TOF = 1.51-2.84 x 10^5 s^{-1}) and quantitative selectivity. Under aprotic or protic conditions, DBTD produces a co-electrocatalytic response with **1** by coordinating *trans* to the site of CO_2 binding and mediating electron transfer from the electrode with quantitative efficiency for CO. This assembly is reliant on through-space electronic conjugation between the π frameworks of DBTD and the bpy fragment of the catalyst ligand, with contributions from dispersive interactions and weak sulfone coordination. The resulting interaction stabilizes a key intermediate in a new aprotic catalytic pathway and lowers the energy of the rate-determining transition state under protic conditions.

Concerns over increasing energy demands and climate change have led to continued interest in molecular electrocatalysis.[1-3] The conversion of CO_2 to value-added products, as part of a carbon neutral (or negative) cycle, is an attractive strategy for addressing the challenges associated with the rising atmospheric CO_2 concentration.[4-9] The electrocatalytic reduction of CO_2 to CO could significantly alter the emissions impact of industrial processes related to Fischer-Tropsch chemistry and syngas, if hydrogen from renewable sources is used.[10-13]

The reduction of CO_2 to CO by molecular electrocatalysts requires the sequential transfer of two electrons and an oxo acceptor (e.g. $2H^+$ or CO_2).[14-15] The general paradigm is for a catalyst to accept electrons from the electrode prior to substrate binding. During energy conversion in living cells, chemical bonds are modified by synergistic systems, like the electron transport chain, which achieve high energy efficiency and selectivity by pairing redox-active moieties with metal centers to direct the flow of reducing equivalents.[16] Analogous reactivity has been translated to only one example of homogenous co-electrocatalytic CO_2 reduction,[17] while similar reactivity is known for other electrocatalytic reactions.[18-21] An alternative for directing electron transfer is through-space electronic conjugation (TSEC), a mechanism of electronic communication between stacked π systems which enables efficient energy and charge transport that has found application in optoelectronic materials and conductance studies of molecular junctions (**Figure 1**).[22-26]

Intrigued by the notion that TSEC could enhance catalytic activity in catalyst-mediator assemblies, we sought to identify a suitable redox mediator (RM) and transition metal complex. We selected dibenzothiophene-5,5-dioxide (DBTD) as the RM (**Figure 1**), which is derived from a petroleum contaminant[27] and has well-defined electrochemical properties at reducing potentials,[28] to pair with a Cr-based catalyst developed in our lab, Cr(^{tbu}dhbpy)Cl(H_2O) (**Figure 1**).[29-30] Herein, we report to our knowledge the only example where TSEC has been used as a key component in a homogeneous co-electrocatalytic reaction. DBTD functions in part to drive electron transfer in an analogous way to RMs used in dye-sensitized solar cells or bioelectrocatalysis, with a more reducing standard reduction potential than the Cr catalyst.[31-32] However, an inner-sphere interaction between the Cr catalyst and DBTD also modifies the potential energy surface of the

reaction, promoting aprotic CO_2 reduction and enhancing kinetic activity in the mechanism of the protic pathway. This co-catalytic behavior is the combined result of weak sulfone coordination to the Cr center, dispersive forces, and TSEC between the RM and ligand backbone of the catalyst.

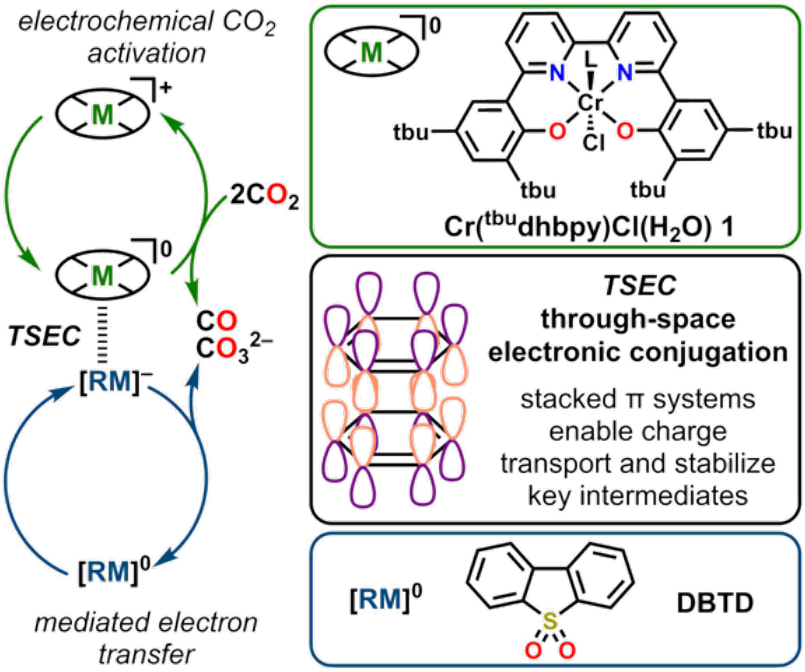

Figure 1. Overview of co-electrocatalytic system with inner-sphere electron transfer based on TSEC between DBTD and Cr(^{tbu}dhbpy)Cl(H_2O) **1**.

Cyclic voltammetry (CV) experiments were carried out in 0.1 M tetrabutylammonium hexafluorophosphate ($TBAPF_6$) with *N,N*-dimethylformamide (*N,N*-DMF) as the solvent. Under argon (Ar) saturation conditions, DBTD displays a reversible redox feature with an $E_{1/2}$ = –2.25 V versus the ferrocenium/ferrocene (Fc^+/Fc) internal standard (**Figure S1**). Control CVs show minimal reactivity with CO_2 or phenol (PhOH) on the CV timescale. As has been established in previous studies,[28] CV analysis and DFT computation under aprotic conditions established that this redox feature is a one-electron process (**see SI**). A control electrolysis experiment was performed with DBTD under CO_2 saturation conditions and again with added PhOH (**Figures S2-S3**): CO and H_2 were detected with low Faradaic efficiencies (FEs) and less than one turnover was achieved based on [DBTD] in both cases (**Table 1**). Under aprotic CO_2 saturation conditions, **1** does not

achieve a single turnover of CO production in electrolysis experiments and no co-products were detected.

The addition of DBTD (2.5 mM) to a solution of **1** (1.0 mM) under Ar saturation conditions suggests no interaction occurs at the $DBTD^{0/-}$ reduction under inert conditions (**Figure S4**). Conversely, under CO_2 saturation conditions this mixture generates a large irreversible increase in current at the $DBTD^{0/-}$ couple, suggestive of a catalytic process (**Figure 2**, blue).[33] *This reactivity is not intrinsic to either component in control reactions*: **1** and DBTD do not individually possess electrocatalytic activity for aprotic CO_2 reduction. Because the Cr catalyst does not present an intrinsic reduction feature near –2.25 V vs Fc^+/Fc, this suggests that DBTD does not act simply as an outer-sphere RM, but rather that the one-electron reduction of DBTD results in the formation of a new adduct that modifies the electronic structure of **1**, enabling co-electrocatalytic CO_2 reduction. It is also worth noting that sulfones are poor ligands with few reports on their coordination chemistry, suggesting that the molecular interaction cannot be exclusively ascribed to a strong dative covalent bond between sulfone and Cr.[34-35]

Importantly, no co-electrocatalytic activity is observed in control experiments with decamethylcobaltocene and **1**, further confirming that outer-sphere electron transfer alone cannot achieve co-electrocatalytic behavior (**Figure S8**). Dibenzothiophene-5-oxide was observed to react with CO_2 in the absence of **1**, rendering it unsuitable for co-electrocatalytic conditions (**Figure S9**). While the experimental and computational data presented here suggest that Cr-sulfone interactions are important, the relatively more basic sulfoxide is incompatible with reaction conditions in the reduced state.

Bulk electrolysis experiments with **1** and DBTD at –2.3 V vs Fc^+/Fc show 91±10% efficiency for CO, with carbonate confirmed as the co-product by NMR, indicating that the reductive disproportionation of CO_2 is occurring (**Tables 1** and **S3**; **Figure S10**).[36] Variable concentration studies were carried out via CV (**Figures S11-S13**), indicating that the catalytic current has a dependence on [DBTD] and [**1**]. Comparable experiments with CO_2 showed a first-order concentration dependence. Since the overall reaction requires two equivalents of CO_2, this observation suggests that one of the CO_2 binding steps is kinetically invisible under catalytic conditions. Varying the concentration of a fixed ratio of DBTD to **1** showed consistent increases in current with sustained irreversibility at the

DBTD reduction potential (**Figure S14**). We note that the complexity of the proposed reaction pathway and overlapping current responses precludes the accuracy of more detailed analyses, but emphasize that in all cases the catalytic current is proportional to the concentration of all components. Further, a shift to positive potentials is observed with increasing [DBTD], consistent with a favorable binding equilibrium under catalytic conditions (**Figure S15**).[33] These shifts are absent under Ar saturation when both components are present (**Figure S16**).

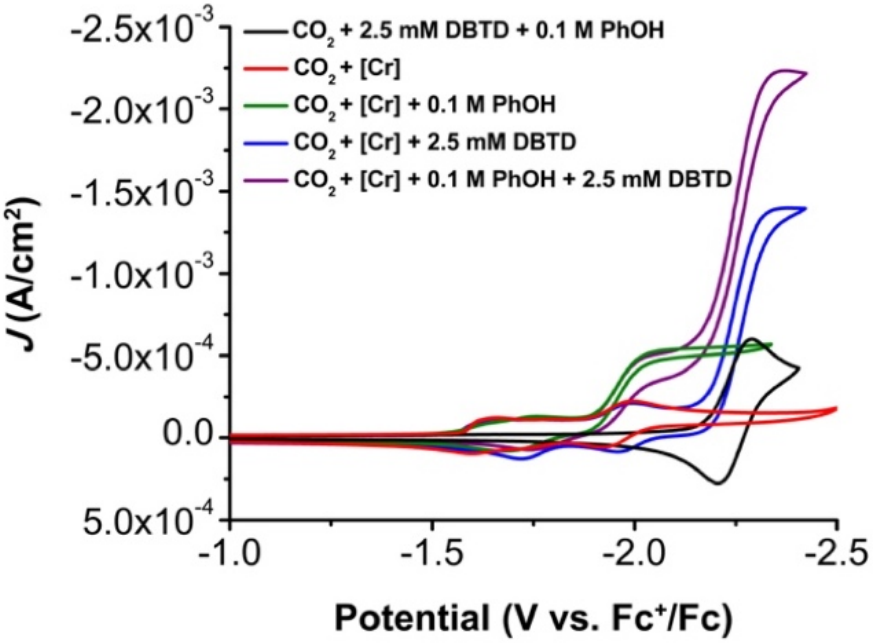

Figure 2. CVs comparing the reactivity of Cr(^{tbu}dhbpy)Cl(H_2O) **1** (1.0 mM) and DBTD under aprotic and protic conditions; 100 mV/s, 0.1 M $TBAPF_6$/DMF.

When 0.1 M PhOH is added to **1** and DBTD under CO_2 saturation, minimal difference compared to identical conditions in the absence of DBTD is observed until ca. −2.10 V vs Fc^+/Fc[29] (**Figure 2**). A comparison of all catalytic conditions indicates that the increase in current density at −2.25 V vs Fc^+/Fc does not correspond to a simple overlay of the independent catalytic responses: PhOH and **1** produce 0.542 mA/cm^2 catalytic current density under CO_2 saturation, **1** and DBTD generate 1.39 mA/cm^2, and the combination of PhOH, DBTD and **1** yield 2.23 mA/cm^2. Bulk electrolysis experiments at –2.3 V vs Fc^+/Fc with **1**, DBTD, and PhOH present 102±14% efficiency for CO (**Figure S4**, **Table 1**). Variable concentration studies were subsequently analyzed to establish kinetic

relationships between **1**, DBTD, PhOH, and CO_2 (**Figures S17-S21**). These data again show that the catalytic current is proportional to the concentration of 1, DBTD, and the combination of the two, as well as PhOH and CO_2.

Table 1. Results from CPE experiments under CO_2 saturation conditions.

Conditions	Potential (V vs Fc^+/Fc)	FE_{CO} (%)	TOF_{CPE} s^{-1}	η (V)	TON_{CO} (w.r.t [1])	TON_{CO} (w.r.t [DBTD])
[Cr]	-2.3	0	-	-	-	-
DBTD	-2.3	32±1	-	-	-	0.90
[Cr] + DBTD	-2.3	91±10	1.51×10^5	0.69	16	3.1
DBTD + PhOH	-2.3	28±1	-	-	-	0.52
[Cr] + PhOH	-2.3	111±14	3.10×10^4	0.11	11.4	-
[Cr] + PhOH + DBTD	-2.3	102±14	2.84×10^5	0.41	29	5.8
[Cr]	-2.7	57±3	-	1.14	0.81	-
[Cr] + PhOH[a]	-2.1	96±8	1.79×10^4	0.11	15[a]	-

* –[Cr] = Cr(^{tbu}dhbpy)Cl(H_2O) **1**. PhOH = 0.6 M [PhOH]. Turnovers correspond to moles of electrons passed in coulometry studies divided by two to account for CO formation. [a] – previously reported results.[29]

Based on our computational model of the intrinsic catalytic cycle of **1**[30] we conducted DFT studies to locate probable reaction pathways under aprotic and protic conditions with DBTD present (**see SI**). We propose the following co-catalytic mechanism under aprotic conditions (**Figure 3**). Beginning from the four-coordinate monoanionic species [Cr(^{tbu}dhbpy)]$^-$ ***i***, CO_2 binding is kinetically accessible in an overall endergonic reaction pathway to produce a mono-CO_2 adduct ***ii*** (**Figures S22-S24**).[29-30] Note that the four-coordinate monoanionic species ***i*** is generated by an overall two-electron reduction of **1**. Although **1** displays no intrinsic electrocatalytic activity under aprotic conditions, the formation of the mono-CO_2 adduct ***ii*** was proposed to be highly reversible and unfavored in our previous mechanistic and computational studies.[29-30] Subsequently, the most likely

pathway in aprotic CO_2 reduction is the binding of a second equivalent of CO_2 to make a bis-CO_2 adduct ***iii*** (**Figure S25**).

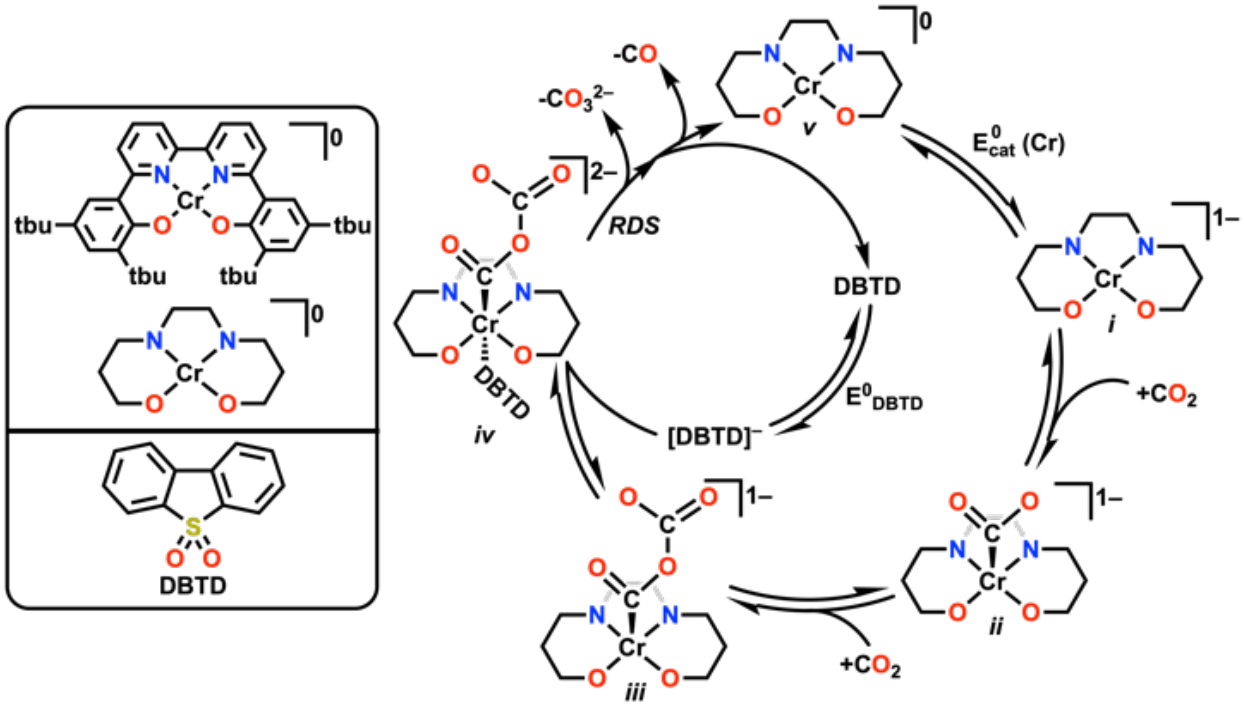

Figure 3. Proposed mechanism for co-electrocatalytic CO_2 reduction by **1** and DBTD under aprotic conditions.

Despite the anticipated Coulombic repulsion, binding of $[DBTD]^-$ in the axial position opposite to the bis-CO_2 fragment in ***iii*** to produce $[Cr(^{tbu}dhbpy)(CO_2CO_2)(DBTD)]^{2-}$ (S = 1) ***iv*** is favorable (–5.5 kcal/mol), relative to DMF coordination (**Figure S26**). We hypothesize that carbonate dissociation from the bis-CO_2 adduct ***iv*** then produces a neutral Cr–CO, from which facile and irreversible CO loss occurs to generate the neutral four-coordinate species ***v*** after DBTD release, completing the cycle.[30] Examination of the electronic structure of $[Cr(^{tbu}dhbpy)(CO_2CO_2)(DBTD)]^{2-}$ ***iv*** through Kohn-Sham orbital projections, spin density plots, and Atoms in Molecules (AIM)[37] analysis suggests that the stability of this species originates in part from the delocalization of the high-energy electron in $[DBTD]^-$ into the bpy fragment of the catalyst via TSEC (**Figures 4** and **S25**).[38-40] This type of interaction between radicals with highly delocalized pi-electrons has been previously referred to as a 'pancake' bond.[41] Including dispersion corrections at the

optimization stage is crucial to obtain reliable molecular geometries[42]: no true minimum for the bimolecular assembly can be located in the S=1 manifold for ***iv*** without accounting for dispersion corrections. Appropriate minima with and without dispersion corrections were located for the higher energy S=2 alternative of ***iv***, allowing an estimated stabilizing effect of ca. 20 kcal/mol for dispersive interactions between the Cr complex and DBTD (**Figure S27**). Thus, while TSEC alters key aspects of the electronic structure relevant to the co-catalytic response, dispersion effects and the formation of a Cr–O bond in the *trans* position to CO_2 binding contribute significantly to adduct formation.

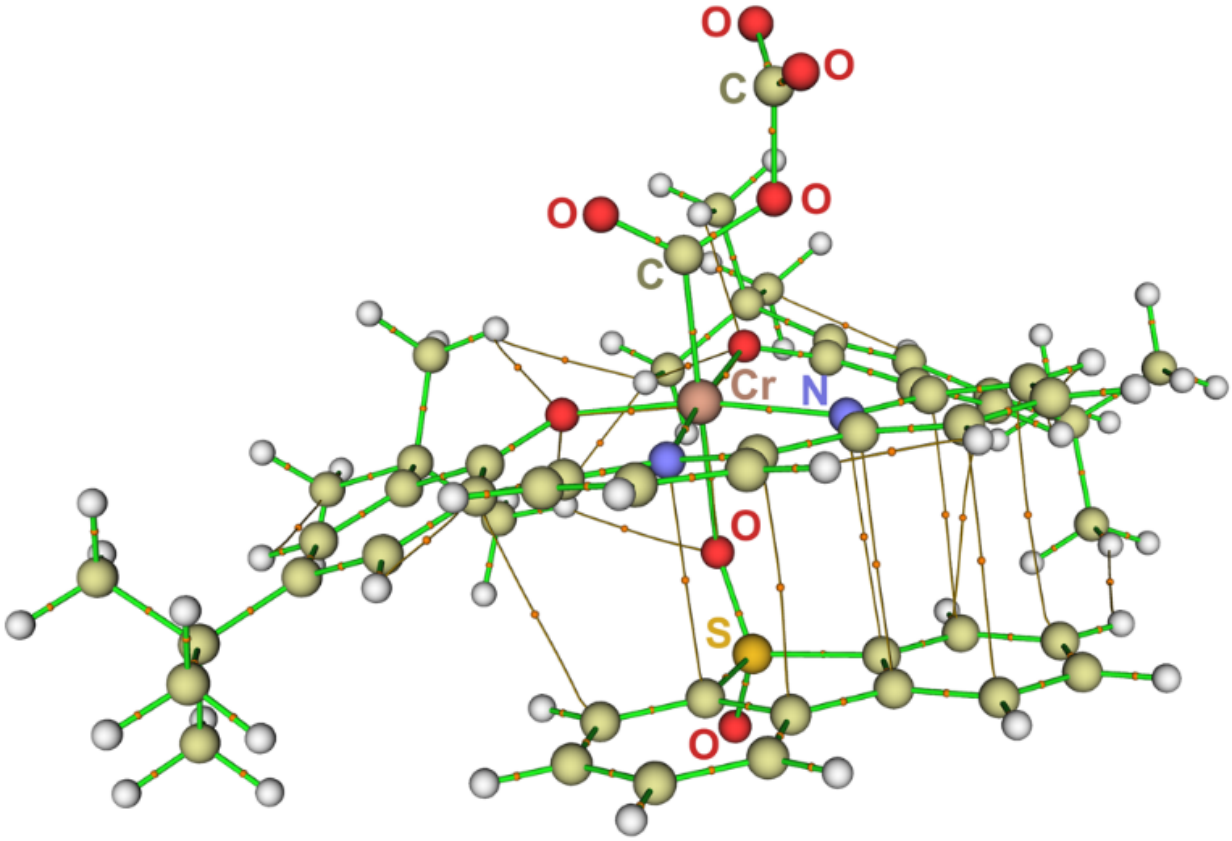

Figure 4. Results of AIM analysis[37] showing (3,-1) bond critical points (bronze lines) between $[DBTD]^-$ and the $[Cr(^{tbu}dhbpy)(CO_2CO_2)]^-$ fragment.[38-40]

The mechanistic possibilities are more complex when PhOH is present (**Figure S28**).[29-30] In the intrinsic electrocatalytic cycle of **1**, the steps depicted in **Figure 3** from ***i*** *to* ***ii*** remain the same. At this point, protonation of ***ii*** by PhOH to form a Cr-CO_2H species is thermodynamically favored.[30] This species is rapidly reduced under catalytic conditions

([Cr-CO_2H]$^{0/-}$ = –1.92 V vs Fc^+/Fc), at which point the TOF-determining C–OH bond cleavage occurs to produce a Cr–CO with free H_2O as a co-product. Experimentally and computationally, loss of CO from this species is rapid.

Because the intrinsic catalytic response of **1** with PhOH present occurs at more positive potentials than DBTD reduction, we cannot exclude $DBTD^-$ functioning as an outer-sphere reductant under these conditions. However, DFT calculations suggest that a viable inner-sphere pathway to increased rates exists. From the six-coordinate monoanionic [Cr-CO_2H]$^-$ species identified previously,[30] replacement of an axial DMF ligand by $DBTD^-$ to create a dianionic species is thermodynamically favorable. Examination of the Kohn-Sham orbitals of the DBTD and $[DBTD]^-$ adducts with [Cr-CO_2H]$^-$ supports the proposal that a pancake bond[41] and Cr–O bond formation are key components for association (**Figure S29**). The transition state for C−OH bond cleavage from [Cr(^{tbu}dhbpy)(CO_2H)(DBTD)]$^{2-}$ is slightly lower than in the absence of the mediator (**Figure S28**). Thus, although this inner-sphere route cannot be assigned as the exclusive source of the enhanced rates observed experimentally, a viable mechanistic pathway exists. Spin density plots are also consistent with pancake bonding and AIM analysis again indicates bond critical points between $[DBTD]^-$ and the bpy fragment of the [Cr-CO_2H]$^-$ complex (**Figure S30**).[38-40]

It is important to emphasize that the formation of a co-electrocatalytic assembly featuring a Cr–O bond is predicted by DFT methods and implied by experimental observation: under aprotic conditions a new catalyst species is required to explain the alternative reactivity of the combined system in comparison to the individual inactivity of DBTD and **1**. Therefore, the best description for the electron transfer between the RM and **1** is an inner-sphere reaction, which makes it unique among reported RMs. Indeed, the existence of an inner-sphere electron transfer pathway involving a non-covalently linked RM and a photoredox catalyst was only recently demonstrated experimentally.[43] Other examples of mediated electron transfer in homogeneous catalysis are proposed to proceed largely through outer-sphere pathways.[44-48]

In conclusion, we report what is, to the best of our knowledge, the only example of an inner-sphere electron transfer RM in a co-electrocatalytic system. The addition of DBTD demonstrates nascent electrocatalytic CO_2 reduction activity under aprotic conditions, at

a potential where **1** has no intrinsic catalytic response in its absence. Substitution of DBTD for decamethylcobaltocene does not result in any co-electrocatalytic activity. Our experimental and computational results indicate that dispersive interactions, TSEC, and weak sulfone coordination are all required to achieve co-electrocatalytic activity enhancement by directing the association of DBTD and **1** for inner-sphere electron transfer to occur. This association creates a co-catalytic assembly with activity for aprotic CO_2 reduction to CO and CO_3^{2-}.

With a proton donor present, the contribution of outer-sphere electron transfer to the kinetic enhancement cannot be ruled out, but substitution of an axial DMF ligand with the reduced RM is also thermodynamically favorable, resulting in a lower energy rate-determining transition state. Pancake bonding[41] has been described in studies of stacking aromatic radicals[49-50] and we propose that this contributes to the viability of an inner-sphere electron transfer pathway between DBTD and **1**. These results suggest that RMs which interact with redox-active ligand frameworks can be a powerful way to alter electrocatalytic mechanisms and improve kinetic rates through inner-sphere electron transfer in a manner competitive with the 'state-of-the-art' (**Figure S31**). Computational and experimental studies to optimize this system are ongoing.

Acknowledgements

The authors thank the University of Virginia for generous funding and institutional support.

Keywords: electrocatalysis • chromium • carbon dioxide fixation• redox mediator • co-catalysis

TOC:

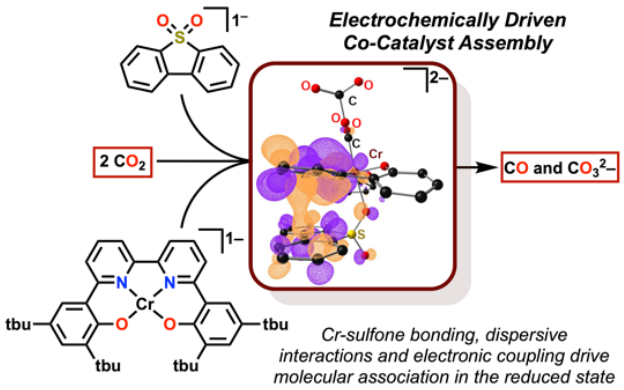

References:

1. DuBois, D. L., Development of Molecular Electrocatalysts for Energy Storage. *Inorg. Chem.* **2014,** *53* (8), 3935-3960.
2. Das, B.; Thapper, A.; Ott, S.; Colbran, S. B., Structural features of molecular electrocatalysts in multi-electron redox processes for renewable energy – recent advances. *Sustainable Energy & Fuels* **2019,** *3* (9), 2159-2175.
3. IPCC *Global Warming of 1.5°C. An IPCC Special Report*; World Meterological Organization: Geneva, Switzerland, 2018.
4. Appel, A. M.; Bercaw, J. E.; Bocarsly, A. B.; Dobbek, H.; DuBois, D. L.; Dupuis, M.; Ferry, J. G.; Fujita, E.; Hille, R.; Kenis, P. J. A.; Kerfeld, C. A.; Morris, R. H.; Peden, C. H. F.; Portis, A. R.; Ragsdale, S. W.; Rauchfuss, T. B.; Reek, J. N. H.; Seefeldt, L. C.; Thauer, R. K.; Waldrop, G. L., Frontiers, Opportunities, and Challenges in Biochemical and Chemical Catalysis of CO2 Fixation. *Chem. Rev.* **2013,** *113* (8), 6621–6658.
5. Aresta, M.; Dibenedetto, A.; Angelini, A., Catalysis for the Valorization of Exhaust Carbon: from CO2 to Chemicals, Materials, and Fuels. Technological Use of CO2. *Chem. Rev.* **2014,** *114* (3), 1709-1742.
6. Morris, A. J.; Meyer, G. J.; Fujita, E., Molecular Approaches to the Photocatalytic Reduction of Carbon Dioxide for Solar Fuels. *Acc. Chem. Res.* **2009,** *42* (12), 1983–1994.
7. Francke, R.; Schille, B.; Roemelt, M., Homogeneously Catalyzed Electroreduction of Carbon Dioxide—Methods, Mechanisms, and Catalysts. *Chem. Rev.* **2018,** *118* (9), 4631-4701.
8. Kinzel, N. W.; Werlé, C.; Leitner, W., Transition Metal Complexes as Catalysts for the Electroconversion of CO2: An Organometallic Perspective. *Angew. Chem., Int. Ed.* **2021,** (n/a), https://doi.org/10.1002/anie.202006988.
9. Kinzel, N. W.; Werlé, C.; Leitner, W., Übergangsmetallkomplexe als Katalysatoren für die elektrische Umwandlung von CO2–eine metallorganische Perspektive. *Angewandte Chemie*, https://doi.org/10.1002/ange.202006988.
10. Jacobs, G.; Davis, B. H., Chapter 5 Conversion of Biomass to Liquid Fuels and Chemicals via the Fischer–Tropsch Synthesis Route. In *Thermochemical Conversion of Biomass to Liquid Fuels and Chemicals*, The Royal Society of Chemistry: 2010; pp 95-124.
11. Seh, Z. W.; Kibsgaard, J.; Dickens, C. F.; Chorkendorff, I.; Nørskov, J. K.; Jaramillo, T. F., Combining theory and experiment in electrocatalysis: Insights into materials design. *Science* **2017,** *355* (6321), eaad4998.
12. Alper, E.; Yuksel Orhan, O., CO2 utilization: Developments in conversion processes. *Petroleum* **2017,** *3* (1), 109-126.
13. Agarwal, A. S.; Rode, E.; Sridhar, N.; Hill, D., Conversion of CO2 to Value-Added Chemicals: Opportunities and Challenges. In *Handbook of Climate Change Mitigation and Adaptation*, Chen, W.-Y.; Suzuki, T.; Lackner, M., Eds. Springer New York: New York, NY, 2014; pp 1-40.
14. Qiao, J.; Liu, Y.; Hong, F.; Zhang, J., A review of catalysts for the electroreduction of carbon dioxide to produce low-carbon fuels. *Chem. Soc. Rev.* **2014,** *43* (2), 631-675.

15. Benson, E. E.; Kubiak, C. P.; Sathrum, A. J.; Smieja, J. M., Electrocatalytic and homogeneous approaches to conversion of CO2 to liquid fuels. *Chem. Soc. Rev.* **2009,** *38* (1), 89-99.
16. Melin, F.; Hellwig, P., Redox Properties of the Membrane Proteins from the Respiratory Chain. *Chem. Rev.* **2020,** *120* (18), 10244-10297.
17. Smith, P. T.; Weng, S.; Chang, C. J., An NADH-Inspired Redox Mediator Strategy to Promote Second-Sphere Electron and Proton Transfer for Cooperative Electrochemical CO2 Reduction Catalyzed by Iron Porphyrin. *Inorg. Chem.* **2020,** *59*, 9270–9278.
18. Anson, C. W.; Ghosh, S.; Hammes-Schiffer, S.; Stahl, S. S., Co(salophen)-Catalyzed Aerobic Oxidation of p-Hydroquinone: Mechanism and Implications for Aerobic Oxidation Catalysis. *J. Am. Chem. Soc.* **2016,** *138* (12), 4186-4193.
19. Landa-Medrano, I.; Lozano, I.; Ortiz-Vitoriano, N.; Ruiz de Larramendi, I.; Rojo, T., Redox mediators: a shuttle to efficacy in metal–O2 batteries. *J. Mat. Chem. A* **2019,** *7* (15), 8746-8764.
20. Liang, Z.; Lu, Y.-C., Critical Role of Redox Mediator in Suppressing Charging Instabilities of Lithium–Oxygen Batteries. *J. Am. Chem. Soc.* **2016,** *138* (24), 7574-7583.
21. Anson, C. W.; Stahl, S. S., Cooperative Electrocatalytic O2 Reduction Involving Co(salophen) with p-Hydroquinone as an Electron–Proton Transfer Mediator. *J. Am. Chem. Soc.* **2017,** *139* (51), 18472-18475.
22. Li, J.; Shen, P.; Zhao, Z.; Tang Ben, Z., Through-Space Conjugation: A Thriving Alternative for Optoelectronic Materials. *CCS Chemistry 1* (2), 181-196.
23. Morisaki, Y.; Chujo, Y., Through-space conjugated polymers consisting of [2.2]paracyclophane. *Polym. Chem.* **2011,** *2* (6), 1249-1257.
24. Bai, M.; Liang, J.; Xie, L.; Sanvito, S.; Mao, B.; Hou, S., Efficient conducting channels formed by the π-π stacking in single [2,2]paracyclophane molecules. *J. Chem. Phys.* **2012,** *136* (10), 104701.
25. Morisaki, Y.; Chujo, Y., Through-Space Conjugated Polymers Based on Cyclophanes. *Angew. Chem., Int. Ed.* **2006,** *45* (39), 6430-6437.
26. Morisaki, Y.; Chujo, Y., "Durch den Raum" konjugierte Cyclophanpolymere. *Angew. Chem.* **2006,** *118* (39), 6580-6587.
27. Breysse, M.; Djega-Mariadassou, G.; Pessayre, S.; Geantet, C.; Vrinat, M.; Pérot, G.; Lemaire, M., Deep desulfurization: reactions, catalysts and technological challenges. *Catal. Today* **2003,** *84* (3), 129-138.
28. Tsai, E. W.; Throckmorton, L.; McKellar, R.; Baar, M.; Kluba, M.; Marynick, D. S.; Rajeshwar, K.; Ternay, A. L., Electrochemistry of thioxanthene, thioxanthone and related compounds in acetonitrile: Substituent effects and correlation of electrochemical behavior with molecular orbital calculations. *Journal of Electroanalytical Chemistry and Interfacial Electrochemistry* **1986,** *210* (1), 45-67.
29. Hooe, S. L.; Dressel, J. M.; Dickie, D. A.; Machan, C. W., Highly Efficient Electrocatalytic Reduction of CO2 to CO by a Molecular Chromium Complex *ACS Catal.* **2020,** *10*, 1146-1151.
30. Moreno, J. J.; Hooe, S. L.; Machan, C. W., A DFT Study on the Electrocatalytic Reduction of CO_2 to CO by a Molecular Chromium Complex. *Inorg. Chem.* **2020**, DOI:10.1021/acs.inorgchem.0c03136.

31. Chen, H.; Simoska, O.; Lim, K.; Grattieri, M.; Yuan, M.; Dong, F.; Lee, Y. S.; Beaver, K.; Weliwatte, S.; Gaffney, E. M.; Minteer, S. D., Fundamentals, Applications, and Future Directions of Bioelectrocatalysis. *Chem. Rev.* **2020,** *120* (23), 12903-12993.
32. Boschloo, G.; Hagfeldt, A., Characteristics of the Iodide/Triiodide Redox Mediator in Dye-Sensitized Solar Cells. *Accounts of Chemical Research* **2009,** *42* (11), 1819-1826.
33. Savéant, J.-M.; Costentin, C., *Elements of Molecular and Biomolecular Electrochemistry: An Electrochemical Approach to Electron Transfer Chemistry*. Wiley: 2019.
34. Dikarev, E. V.; Becker, R. Y.; Block, E.; Shan, Z.; Haltiwanger, R. C.; Petrukhina, M. A., The First Coordination Complexes of Selenones: A Structural Comparison with Complexes of Sulfones. *Inorg. Chem.* **2003,** *42* (22), 7098-7105.
35. Cotton, F. A.; Felthouse, T. R., Crystal and molecular structure of tetrakis(trifluoroacetato)bis(dimethyl sulfone)dirhodium(II). A compound with axially coordinated sulfone ligands. *Inorg. Chem.* **1981,** *20* (8), 2703-2708.
36. Nichols, A. W.; Chatterjee, S.; Sabat, M.; Machan, C. W., Electrocatalytic Reduction of CO2 to Formate by an Iron Schiff Base Complex. *Inorg. Chem.* **2018,** *57* (4), 2111-2121.
37. Bader, R. F. W., *Atoms in Molecules: A Quantum Theory*. Oxford University Press: Oxford, England, 1995.
38. Garcia-Yoldi, I.; Miller, J. S.; Novoa, J. J., Structure and Stability of the [TCNE]22- Dimers in Dichloromethane Solution: A Computational Study. *J. Phys. Chem. A* **2007,** *111* (32), 8020-8027.
39. Garcia-Yoldi, I.; Miller, J. S.; Novoa, J. J., [Cyanil]22− dimers possess long, two-electron ten-center (2e−/10c) multicenter bonding. *Phys. Chem. Chem. Phys.* **2008,** *10* (28), 4106-4109.
40. Mota, F.; Miller, J. S.; Novoa, J. J., Comparative Analysis of the Multicenter, Long Bond in [TCNE]·− and Phenalenyl Radical Dimers: A Unified Description of Multicenter, Long Bonds. *J. Am. Chem. Soc.* **2009,** *131* (22), 7699-7707.
41. Kertesz, M., Pancake Bonding: An Unusual Pi-Stacking Interaction. *Chem. – Eur. J.* **2019,** *25* (2), 400-416.
42. Lyngvi, E.; Sanhueza, I. A.; Schoenebeck, F., Dispersion Makes the Difference: Bisligated Transition States Found for the Oxidative Addition of Pd(PtBu3)2 to Ar-OSO2R and Dispersion-Controlled Chemoselectivity in Reactions with Pd[P(iPr)(tBu2)]2. *Organometallics* **2015,** *34* (5), 805-812.
43. Kellett, C. W.; Swords, W. B.; Turlington, M. D.; Meyer, G. J.; Berlinguette, C. P., Resolving orbital pathways for intermolecular electron transfer. *Nat. Comm.* **2018,** *9* (1), 4916.
44. Lennox, A. J. J.; Nutting, J. E.; Stahl, S. S., Selective electrochemical generation of benzylic radicals enabled by ferrocene-based electron-transfer mediators. *Chem. Sci.* **2018,** *9* (2), 356-361.
45. Zhu, L.; Xiong, P.; Mao, Z.-Y.; Wang, Y.-H.; Yan, X.; Lu, X.; Xu, H.-C., Electrocatalytic Generation of Amidyl Radicals for Olefin Hydroamidation: Use of Solvent Effects to Enable Anilide Oxidation. *Angew. Chem., Int. Ed.* **2016,** *55* (6), 2226-2229.

46. Zhu, L.; Xiong, P.; Mao, Z. Y.; Wang, Y. H.; Yan, X.; Lu, X.; Xu, H. C., Electrocatalytic generation of amidyl radicals for olefin hydroamidation: use of solvent effects to enable anilide oxidation. *Angew. Chem.* **2016,** *128* (6), 2266-2269.
47. Wu, Z.-J.; Xu, H.-C., Synthesis of C3-Fluorinated Oxindoles through Reagent-Free Cross-Dehydrogenative Coupling. *Angew. Chem., Int. Ed.* **2017,** *56* (17), 4734-4738.
48. Wu, Z. J.; Xu, H. C., Synthesis of C3-Fluorinated Oxindoles through Reagent-Free Cross-Dehydrogenative Coupling (Angew. Chem. 17/2017). *Angew. Chem.* **2017,** *129* (17), 4703-4703.
49. Kiguchi, M.; Takahashi, T.; Takahashi, Y.; Yamauchi, Y.; Murase, T.; Fujita, M.; Tada, T.; Watanabe, S., Electron Transport through Single Molecules Comprising Aromatic Stacks Enclosed in Self-Assembled Cages. *Angew. Chem., Int. Ed.* **2011,** *50* (25), 5708-5711.
50. Kiguchi, M.; Takahashi, T.; Takahashi, Y.; Yamauchi, Y.; Murase, T.; Fujita, M.; Tada, T.; Watanabe, S., Electron transport through single molecules comprising aromatic stacks enclosed in self-assembled cages. *Angew. Chem.* **2011,** *123* (25), 5826-5829.